Coexistence Analysis of Co-located BLE and IEEE 802.15.4 TSCH Networks

Hamideh Hajizadeh, Majid Nabi, *Member, IEEE*, Maik Vermeulen, and Kees Goossens, *Member, IEEE*

***Abstract*— Bluetooth Low Energy (BLE) and IEEE 802.15.4 Time-Slotted Channel Hopping (TSCH) are widely used low-power standard technologies developed for short-range communications in the internet-of-things. In many applications, BLE and TSCH networks may be deployed in the vicinity of one another, which may lead to Cross Technology Interference (CTI) influencing each other's performance. Both technologies utilize channel hopping to alleviate the impact of external interferences. However, having a model to quantitatively estimate the performance of coexisting TSCH and BLE networks and analyze the role of networks' configuration settings is still an open problem. To address this, we provide a probabilistic analysis of collision-free communication of coexisting BLE and TSCH networks. Moreover, a fast coexistence simulation model is developed that computes the ratio of collision-free transmissions. This model is used to investigate how the performance of the coexisting networks may deviate from the results of the probabilistic analysis. It gives the designers a proper estimation of the worst case performance degradation due to such coexistence. It is shown that severity of the impact of coexisting BLE-TSCH networks on one another depends on the setup configurations and the relative timing of the two networks. The results show that these two technologies can coexist well with collision-free ratios of more than 92.58% and 96.29% in the tested configurations for TSCH and BLE, respectively.**

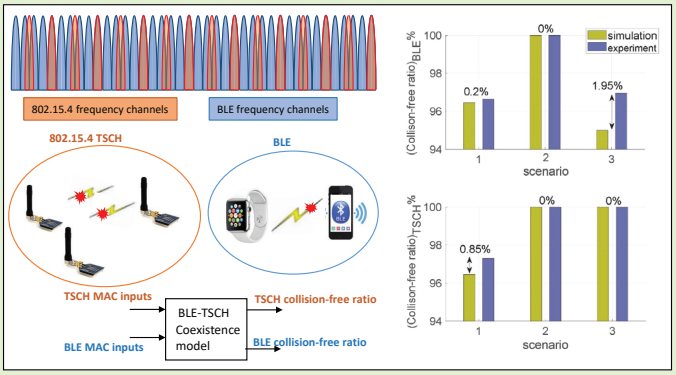

***Index Terms*— IEEE 802.15.4, TSCH, BLE, Coexistence, Simulation model, IoT**

I. Introduction

WIRELESS Sensor Networks (WSNs) are growing as an appealing technology with the rapid development of wireless technology and embedded sensors. Several communication technologies have been developed for WSNs to support various types of applications with different demands. Among them, low-power standards have attracted much interest in power-constrained WSNs. Bluetooth Low Energy (BLE) [1] and IEEE 802.15.4 [2] are two low-power wireless communication standards with a huge number of applications such as smart cities, environmental monitoring, healthcare, smart buildings, and in-vehicle networks [3].

Manuscript received xxx; accepted xxx. Date of publication xxx; date of current version xxx. This work was supported by the SCOTT European project (www.scott-project.eu), that has received funding from the Electronic Component Systems for European Leadership Joint Undertaking under grant agreement No 737422. (Corresponding author: Hamideh Hajizadeh)

H. Hajizadeh and K. Goossens are with the Department of Electrical Engineering, Eindhoven University of Technology, 5600 MB Eindhoven, The Netherlands (e-mail: h.hajizadeh@tue.nl; k.g.w.goossens@tue.nl)

M. Nabi is with the Department of Electrical Engineering, Eindhoven University of Technology, 5600 MB Eindhoven, The Netherlands, and also with the Department of Electrical and Computer Engineering, Isfahan University of Technology, Isfahan 84156-83111, Iran (e-mail: m.nabi@tue.nl).

M. Vermeulen was with the Department of Electrical Engineering, Eindhoven University of Technology, 5600 MB Eindhoven, The Netherlands.

The IEEE 802.15.4 standard specifies Physical (PHY) and Medium Access Control (MAC) layers for low-power and low-cost wireless communications, operating in the unlicensed 2.4 GHz ISM frequency band. The Time-Slotted Channel Hopping (TSCH), as a MAC operational mode of this standard, uses time-slotted communications to provide collision-free channel access, and frequency channel hopping to mitigate external interferences and multipath fading. BLE has been introduced by the Bluetooth Special Interest Group (Bluetooth SIG) in 2010 as a low-power communication technology. Compared to classic Bluetooth, BLE aims at providing considerably reduced power consumption and cost while maintaining a similar communication range. BLE uses channel hopping in the 2.4GHz ISM band to combat the impact of interference and multi-path fading effects.

Because of widespread use of BLE and TSCH technologies in many Internet-of-Things (IoT) applications, there is a good chance that networks based on these standards co-locate in some applications. Automotive, smart building, and healthcare are examples. For instance, a health monitoring WSN is developed in [4], in which BLE is used to collect data from wearable sensors while TSCH is used as the network backbone for propagating data samples of body sensors as well as ambient sensors. Since both technologies operate in the same ISM frequency band, the impact of their communications on each other may be a great concern in such scenarios.

Coexistence of TSCH and BLE with other technologies operating in the same frequency band such as Wi-Fi has been studied in the literature. Authors in [5] have shown that both technologies can coexist with Wi-Fi with an acceptable performance. However, the coexistence between TSCH and BLE is still an open problem to be investigated. The application designers are in particular interested to have an estimation about the severity of the influence of these networks on each other when they are deployed in the interference range of each other. Some have tried to better understand the impact of communications in such networks on each other in the physical layer (e.g., [6]). Also, mechanisms to alleviate the impact have been developed to reduce the probability of collisions [7]. However, a detailed study of the coexistence behavior of these two channel hopping networks in the MAC layer is lacking. Such an investigation can provide an insight into the performance of these networks when they operate in the vicinity of each other.

A prerequisite for such investigation is having a scalable and fast coexistence simulation model that can estimate the inter-network collisions in time and frequency domains for any given configuration of the two networks. The network simulators such as Cooja [8] or OMNeT++ [9] simulate details of different layers in the protocols stacks including packet transmission flow with all the headers and trailers of various layers. Because of that, such discrete event-driven simulators are usually very slow in simulating a single network configuration for a relatively high number of packet exchanges. For the coexistence investigation, we need to simulate many configurations with different random patterns to have statistically reliable results and to be able to catch corner cases. Thus, to enable such Monte-Carlo simulations, we developed a BLE-TSCH coexistence simulator in a high abstraction level that can be fed with any number of TSCH and BLE networks and their configuration settings as its inputs, and report the number of collisions from the perspective of the MAC layer in a very short time. It is actually because we are only interested in detecting the frequency and time overlaps, not actually implementing real packet exchanges and protocol implementations. Accordingly, the contributions of this paper are as follows.

- We analyze the probabilities of overlap in frequency and time domains for coexisting TSCH and BLE networks. Such probabilistic analysis reveals that the probability of having no overlap in time and frequency domains for a pair of packets transmitted in TSCH and BLE is considerably high which leads to a high probability of collision-free coexistence.
- A BLE-TSCH coexistence simulation framework is developed. In the first phase, we develop two separate simulation models for channel occupancy over time for TSCH and BLE protocols in the MAC layer. Then, these models are integrated into a coexistence simulation model, which analyzes possible collision scenarios and outputs collision-free ratios of both networks.
- The proposed simulation model is used to perform Monte-Carlo simulations to investigate the performance of co-located TSCH and BLE networks in various scenarios. In particular, the worst-case coexistence is of our interest as it reveals to what extent such networks can influence each other.

The rest of the paper is organized as follows. A review of the essential background about TSCH and BLE is provided in Section II. Section III reviews the relevant research focusing on coexistence of wireless protocols. Section IV analyzes the collision-free probability for coexisting TSCH and BLE networks in the MAC layer. Section V presents the developed BLE-TSCH coexistence simulator. The experimental setup and the model verification results are discussed in Section VI. Section VII investigates the worst-case coexistence scenario using the developed model. Section VIII studies the impact of clock drift on the coexistence performance. Section IX concludes.

II. Background

A. IEEE 802.15.4 TSCH

The IEEE 802.15.4 standard mainly operates in the 2.4 GHz ISM band with O-QPSK+DSSS as its main PHY layer modulation scheme. It defines 16 frequency channels in this band each with 2 MHz bandwidth and a channel spacing of 5 MHz with data rate of 250 Kbps. TSCH is one of the MAC operational modes of the standard, implementing time-slotted channel access with a channel hopping mechanism. The time-slotted channel access provides collision-free communications, which in turn improves the bandwidth efficiency in dense networks and makes the network performance more predictable. In TSCH, communication between sensor nodes occurs in timeslots, wherein a node can transmit a data packet and receive its Acknowledgment (Ack). Fig. 1 illustrates the structure of a timeslot in TSCH. Sensor nodes use a synchronization mechanism to align their timeslots. To compensate small misalignments caused by clock drifts, a guard time is designed at the beginning of each timeslot. A number of timeslots are grouped together to create a slotframe, which is repeated over time periodically. A timeslot may be exclusively assigned to a node for its contention-free packet transmission, or it may be shared to be accessed by multiple links via a slotted CSMA-CA mechanism to avoid repeated collisions.

The channel hopping mechanism of TSCH improves the communication reliability by mitigating the impact of multi-path fading and external interference. For one transmission between a pair of transmitting and receiving nodes, the frequency channel (f) is calculated as follows.

$$f = HSL[(ASN + channel\ offset)\ mod\ |HSL|] \qquad (1)$$

where ASN is the absolute slot number, a globally synchronized parameter indicating the number of timeslots elapsed from the start of the network. HSL is the channel hopping sequence list, $|HSL|$ is the number of channels that are used for channel hopping, and *channel offset* is a number in the range $[0, |HSL| - 1]$ to allow parallel transmissions in the network.

B. Bluetooth Low Energy

Like in IEEE 802.15.4, BLE operates in the ISM frequency band (the 2.400–2.4835 GHz band), but with a different set

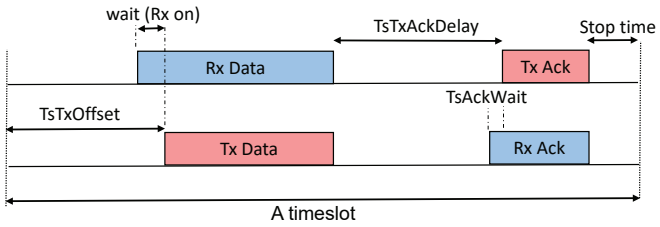

Fig. 1. Structure of a timeslot in IEEE 80215.4 TSCH

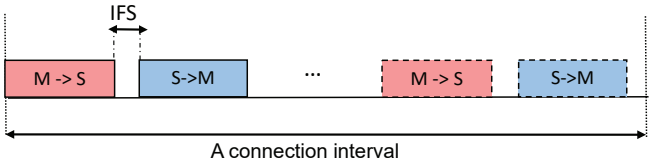

Fig. 2. Packet exchanges in a BLE connection interval. One or more packet transmission can happen in each connection interval.

of channels. BLE PHY layer divides the 2.4 GHz ISM band into 40 back-to-back channels of 2 MHz bandwidth. Within a channel, data is transmitted using the GFSK modulation with a bit rate of 1 Mbps (with an option of 2 Mbps in BLE 5 [10]). The link layer of the BLE stack is responsible for advertising, scanning, and creating a connection between two nodes. Three channels are dedicated to advertising and scanning, while the other 37 channels are defined as data channels to be used for peer-to-peer data communications. In the connection state, the device that initiates the connection is called the master, and the device accepting the connection is called the slave. The link layer of BLE stack runs a channel-selection algorithm for channel hopping in the connection state. The frequency channel (f) for data communication in the connection state is derived as follows.

$$f = ChM[(LUC + hI)\ mod\ |ChM|], \tag{2}$$

where ChM is the channel map representing the available data channels for channel hopping, hI is the hop increment, and LUC is the last unmapped channel. Both ChM and hI are provided by the master node in the connection request message, when initiating a connection. The hI is randomly selected by the master node as a number between 5 and 16, while LUC is initialized to zero, and afterwards is updated by the algorithm, having LUC from the last step.

Data transfer in a BLE network is mainly peer-to-peer, which is done in periodic time intervals called connection intervals. Fig. 2 shows the data transfer model over time in the connection state. During each connection interval, the master first transmits a packet, indicating the beginning of the event. Then, one or more packets can be exchanged by the master and slave during the connection intervals. The duration of the connection interval depends on the amount of traffic that has to be exchanged and is controlled by the master. The time space between two consecutive packets (shown in Fig. 2) is called Inter Frame Spacing (IFS) which is 150 μs according to the BLE specification.

III. Related Work

Since the 2.4 GHz ISM band is used by many wireless technologies such as Bluetooth, IEEE 802.15.4, and WiFi, the coexistence between these technologies attracted broad interests [5], [6], [11]–[19] in the research community. Here, we review the relevant studies in which Bluetooth or IEEE 802.15.4 networks are involved.

NXP semiconductors provides an application note [17], in which the coexistence of the single channel modes of the IEEE 802.15.4 with other protocols operating at 2.4 GHz band is studied in PHY layer. The authors survey empirical data and analytical studies for the coexistence of the IEEE 802.15.4 in the 2.4 GHz with Wi-Fi, classic Bluetooth, and microwave ovens. They conclude that the coexistence of the single channel modes of the IEEE 802.15.4 with Wi-Fi and classic Bluetooth networks leads to an acceptable performance, if the there are either enough spacial spacing or frequency separation. Accordingly, they propose several methods to improve their coexistence such as channel selection, and physical separation. These findings are further backed up in [18], in which authors investigate the coexistence of the single channel modes of the IEEE 802.15.4 and BLE through packet error rate tests. Their tests are performed in the presence of external interferences in the 2.4 GHz, i.e., Wi-Fi routers, IEEE 802.15.4 networks, and Bluetooth devices. It is shown that connection interval of BLE should be carefully set to achieve a better performance of both interfering networks.

R. Natarajan et al. [6] analyze the coexistence between BLE, single channel modes of the IEEE 802.15.4 and WiFi in the PHY layer. They present a mathematical analysis of the spatial, temporal and frequency parameters of the impact of interference on the packet error rate of either networks. Furthermore, they extend their investigation of the coexistence to the MAC layer through experimental setups. The most significant conclusion of this paper is that BLE is affected more by IEEE 802.15.4, than vice versa, since IEEE 802.15.4 employs DSSS modulation resulting in a higher process gain, but longer occupancy of the channel than BLE due to its lower data rate.

In spite of many studies on the coexistence of the single channel modes of IEEE 802.15.4 and BLE, there is a lack of study on the coexistence of IEEE 802.15.4 TSCH and BLE as two channel hopping technologies. [7], [20] are the only two studies devoted to the coexistence between BLE and TSCH networks. In [7], authors propose a cooperative solutions to improve the coexistence of BLE and TSCH. The solution is to unite the BLE and TSCH networks into a centrally coordinated system, and uses a scheduling matrix to predict and resolve the collisions. Although, their solution can improve the performance of the coexistence, it is still unknown how much the performance degrade when these networks coexist. [20] experimentally research the performance of the coexistence between TSCH and BLE for limited number of settings. However, the experimental setups are limited and do not provide a complete view of the coexistence in different scenarios.

Detailed evaluation of the coexistence performance for various settings of TSCH and BLE networks are essential for

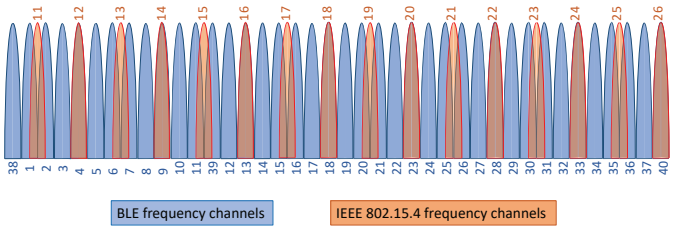

Fig. 3. Frequency channels of IEEE 802.15.4 and BLE

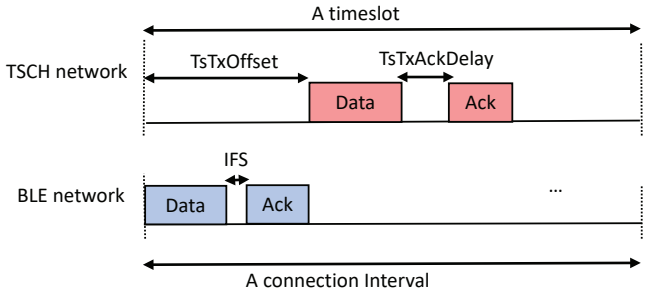

Fig. 4. A scenarios that TSCH and BLE packets do not overlap in time

the networks designers to get an insight about the performance of the networks. To the best of our knowledge, we present here the first coexistence analysis and a simulation model for co-located TSCH and BLE networks in the MAC layer. This simulation model is then used to perform extensive Mote-Carlo simulations in various scenarios to get a proper understanding of the performance of BLE and TSCH networks when they coexist.

IV. Coexistence Probabilistic Analysis

Collision between packet transmissions of two wireless technologies can occur when they overlap in three domains simultaneously: space, time, and frequency. Having co-located TSCH and BLE networks, we need to investigate overlap only in frequency and time domains. In the following, a probabilistic analysis of overlap in the frequency and time domains are separately presented. Then, we analyze collision-free probability through overlap analysis in the frequency and time domains when TSCH and BLE networks coexist.

A. Frequency overlap analysis

Fig. 3 shows how BLE and TSCH frequency channels overlap. Depending on the selected channel by the transmitters of TSCH and BLE, the following scenarios may happen:

Non-overlapped frequency channels: This represent the best scenario, in which the frequency channels selected by the TSCH and BLE do not overlap. (e.g., channel 5 of BLE and channel 15 of TSCH).

Partially-overlapped frequency channels: This scenario represents the situation wherein the selected frequency channels of the transmitters of both technologies partially overlap (e.g., 1MHz overlap for channel 11 of BLE and channel 15 of TSCH).

Fully-overlapped frequency channels: This scenario represents the worst situation wherein the frequency channels of the transmitters of both technologies fully overlap (e.g., channel 23 of BLE and channel 20 of TSCH).

In the two latter scenarios, the transmitted packets of two networks collide if their transmission durations overlap. Let $ChOv$ be a subset of BLE frequency channels ($ChOv \subset ChM$) which overlap (fully or partially) with one of the TSCH frequency channels. We denote $P_{\bar{c}}^{f}$ as the probability of no overlap in frequency domain for a pair of packets transmitted in TSCH and BLE. It is calculated as follows.

$$P_{\bar{c}}^{f} = (1 - \frac{|ChOv|}{|ChM|}) + \frac{|ChOv|}{|ChM|} \times (1 - \frac{1}{|HSL|}) \qquad (3)$$

where $|.|$ denotes the cardinality of the sets. $(1 - \frac{|ChOv|}{|ChM|})$ is the probability that BLE does not transmit in an overlapped frequency channels while the term $\frac{|ChOv|}{|ChM|} \times (1 - \frac{1}{|HSL|})$ is the probability that BLE transmits in one of the overlapped frequency channels and TSCH does not use that channel for transmission. When BLE and TSCH use all available channels for transmissions, $|ChM| = 37$ and $|HSL| = 16$, then $|ChOv| = 22$ and $P_{\bar{c}}^{f} = 0.96$, which indicates high probability of no overlap in the frequency domain.

B. Time overlap analysis

In TSCH and BLE networks, a node does not occupy all the time of a timeslot and connection interval, according to the time structure shown in Fig. 1 and Fig. 2. It means that if two networks transmit in the overlapped frequency channels, there are still chances of having no overlap in time, leading to collision-free communication of the coexisting networks. As an example, Fig. 4 illustrates a case in which the packet and Ack transmission of the two networks interleave with one another. This may happen because of specific time-offset (Δ) between two networks and/or very short packets, which are common in sensor networks.

To show the probability of interference-free communications of two coexisting networks in time, we use the convolution of the time structure of a timeslot and a connection interval over all possible values of the time-offset [21]. The convolution operation provides a cross-correlation function between the timeslot and connection interval in the two networks. Hence, the convolution indicates the time durations in which the data or Ack packet transmissions in the two networks overlap. Data packet lengths of TSCH and BLE (L_{TSCH}^{d}, L_{BLE}^{d}), Ack packet length (L_{TSCH}^{a}, L_{BLE}^{a}), the number of packets transmitted within the connection interval ($PPCI$), duration of TSCH timeslot (T_{ts}), and the connection interval (T_{ci}) determine the output of the convolution function. Let $Conv$ be the convolution function of a timeslot (TS) and a connection interval (CI), which is calculated as follows.

$$Conv(t) = (TS * CI)(t) = \int_{0}^{T_{ts}+T_{ci}} TS(\tau)\ CI(t-\tau)d\tau \qquad (4)$$

where $TS(t)$ and $CI(t)$ are rectangular pulses with amplitude 1, representing signal transmission in a timeslot and a connection interval, respectively. The time durations of amplitude 1 of $TS(t)$ and $CI(t)$ depend on data and Ack packet length of TSCH and BLE, and data rate of these networks. Here, we

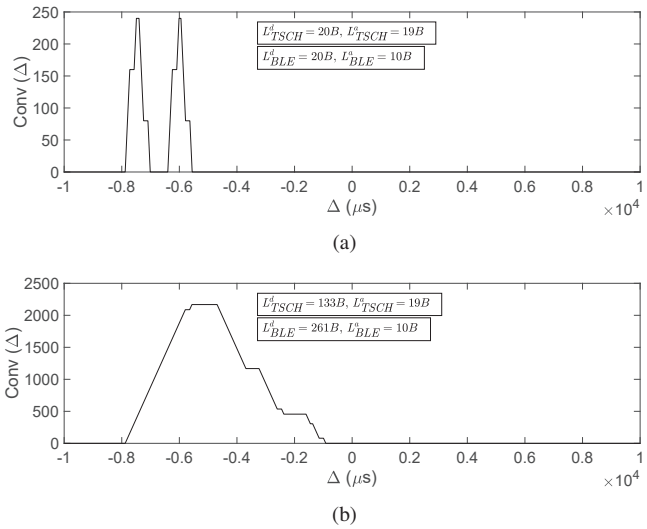

Fig. 5. Convolution (overlap ratio in time) results for different packet length transmission in overlapped frequency channel over different $\boldsymbol{\Delta}$, $T_{ci} = T_{ts} = \mathbf{10}ms$

use 250Kbs, and 1Mbs as TSCH and BLE data rates. Since the convolution operation slides the two input functions over one another in the specified range, it examines all possible time-offsets between the networks. Sliding the two functions over one another in the range $[0\ T_{ts} + T_{ci}]$ is translated in to time-offset in the range of $\Delta = [-T_{ci}\ T_{ts}]$.

Fig. 5 shows the convolution results representing overlap in time when TSCH and BLE networks transmit in overlapping frequency channel with two different set of data packet lengths. As seen, the probability of collision-free communication of two networks depends on the packet lengths, and time-offset between the networks. Then, the probability of no overlap of two coexisting networks in time domain for given Δ ($P^t_{\bar{c}|\Delta}$) is calculated as,

$$P^t_{\bar{c}|\Delta} = F(Conv(t)|t = \Delta), \tag{5}$$

where,

$$F(x) = \begin{cases} 0, & x = 0 \\ 1, & otherwise \end{cases} \tag{6}$$

For example, in the scenario stated in Figure 5(a), $P^t_{\bar{c}|\Delta}$ is 1 if $-7.88ms \leq \Delta \leq -7ms$, or $-6.4ms \leq \Delta \leq -5.55ms$, otherwise it is zero. Similarly, for the longest data packets transmitted by TSCH and BLE (stated in Figure 5(b)), $P^t_{\bar{c}|\Delta}$ is 1 if $-7.88ms \leq \Delta \leq -0.9ms$, otherwise it is zero. Since the coexisting networks are independent and asynchronous, Δ uniformly distributed in the range $[-T_{ci}\ T_{ts}]$. Then, the average probability of no overlap of a pair of packets transmitted in TSCH and BLE in time domain ($P^t_{\bar{c}}$), is calculated as,

$$P^t_{\bar{c}} = \frac{1}{T_{ci} + T_{ts}} \times \int_0^{T_{ci}+T_{ts}} F(Conv(t))dt. \tag{7}$$

From (7), $P^t_{\bar{c}}$ is calculated as 0.90, and 0.65 for the data packet lengths stated in Figures 5(a), and 5(b), respectively. It shows that there is still a considerable chance of collision-free coexistence even when transmissions in the two networks overlap in the frequency domain.

C. Collision analysis in the MAC layer

Here, we intend to analyze the probability of collision-free communications when co-located TSCH and BLE networks coexist. A collision in the MAC layer occurs between these networks when their transmissions overlap in time and frequency simultaneously. Let $P_{\bar{c}}$ be the probability of collision-free transmission for a pair of packets transmitted in TSCH and BLE, which can be calculated as follows.

$$P_{\bar{c}} = 1 - (1 - P^t_{\bar{c}}) \times (1 - P^f_{\bar{c}}) \tag{8}$$

where $P^f_{\bar{c}}$ and $P^t_{\bar{c}}$ are given by (3) and (7), respectively. For the longest data packets transmitted in TSCH and BLE, $P^t_{\bar{c}}$ is 0.65. If both networks use all available channels for channel hopping $P^f_{\bar{c}}$ is 0.96. Thus, $P_{\bar{c}} = 0.98$.

Note that, $P^f_{\bar{c}}$ is calculated for a pair of packets transmitted in TSCH and BLE. If successive packets are transmitted in both networks, the probability of no overlap in the frequency domain will be different. It depends on the channel hopping parameters of TSCH and BLE like *hI*, *channel offset*, frequency channels used by the previous packets, and the frequency channels order in *ChM* and *HSL*. Hence, many possible scenarios can happen for successive packet transmissions in TSCH and BLE, which requires evaluation of many scenarios (e.g., Monte-Carlo simulations) to find the collision-free probability. To tackle this problem, we present a fast simulation model, which models the details of time and frequency behaviour of both networks to calculate collision-free ratio for any configuration considering sufficiently many packet transmissions. Such a model is a beneficial tool for network designers to derive the worst-case scenario of the coexistence through evaluation of all scenarios, and develop mechanisms to avoid from getting trapped into worst-case scenarios.

V. BLE-TSCH Coexistence Simulator

In this section, we first develop simulation models of channel occupancy over time for both TSCH and BLE independently. Then, the derived models are integrated into a BLE-TSCH coexistence simulation model whose goal is to find out collisions and derive collision-free ratios for TSCH and BLE networks. It is assumed that data packet transmission is performed in each timeslot in the TSCH network. It may be done by a single transmitter or several transmitters. In BLE, one or more packets are transmitted in each connection interval by the master or slave nodes. To have a fast simulator, the details of the technology standards in transient states such as connection establishment are not simulated. The focus is on the steady state to extract the exact time and frequency of packet transmissions in the involved networks.

A. TSCH time-frequency model

Here we develop a model that simulates the TSCH behavior in terms of frequency and time of packet transmissions. The model uses the simulation time window denoted by T_{sim}, and the time resolution as δ. Moreover, it uses the TSCH network's configurations listed in Table I. We discretize T_{sim} with the resolution of δ, and scan T_{sim} with steps of length δ to

TABLE I
INPUTS OF TSCH MODEL

Notation	Meaning
T_{sim}	Simulation time
δ	Time resolution of the results
L^d_{TSCH}	Data packet length of TSCH in PHY layer [bytes]
L^a_{TSCH}	Ack packet length of TSCH in PHY layer [bytes]
T_{tsl}	Timeslot duration
HSL	Hopping sequence list of TSCH
ASN	TSCH ASN number (timeslot counter)
Channel Offset	Channel offset of TSCH

TABLE II
INPUTS OF BLE MODEL

Notation	Meaning
T_{sim}	Simulation time
δ	Time resolution of the results
PPCI	Number of packets per connection interval
L^d_{BLE}	Data packet length in PHY layer [bytes]
L^a_{BLE}	Ack packet length in PHY layer [bytes]
IPS	Time spacing between packets
ChM	List of used data channels
hI	Hop increment, a random number in [5,16]
T_{ci}	Connection interval duration

determine frequency channels and exact time of data and Ack packet transmissions in each timeslot of the TSCH network. Let $TSCH_f$ and $TSCH_{tx}$ be two vectors having with $\lfloor T_{sim}/\delta \rfloor$ elements defined as follows.

$$\begin{aligned} &TSCH_f = [f], \quad 11 \leq f \leq 26 \\ &TSCH_{tx} = [indx], \quad indx = [0, i_d, i_a] \end{aligned} \tag{9}$$

where element k $(1 \leq k \leq \lfloor T_{sim}/\delta \rfloor)$ of $TSCH_f$ indicates the frequency channel used for transmission in time $k \times \delta$ in case of transmission of data or Ack packets, otherwise it is zero. The element k $(1 \leq k \leq \lfloor T_{sim}/\delta \rfloor)$ of $TSCH_{tx}$ indicates whether there is a data or Ack packet transmission happening at time $k \times \delta$. The element k $(1 \leq k \leq \lfloor T_{sim}/\delta \rfloor)$ of $TSCH_{tx}$ is i_d, or i_a, if data, or Ack is being transmitted at time $k \times \delta$, respectively, otherwise it is zero.

According to the timing structure of TSCH shown in Fig. 1, in each timeslot after *TsTxOffset*, the transmitter node transmits its data packet in the selected channel. TSCH CCA is assumed to be disabled, as CCA is optional and accurate CCA modeling would require PHY layer analysis, which is not in the scope of this paper. The time duration in which the transmitter occupies the frequency channel for data packet transmission in TSCH is denoted by T^d_{TSCH}, which is calculated as

$$T^d_{TSCH} = \frac{L^d_{TSCH} \times 8}{R_{TSCH}} \tag{10}$$

where R_{TSCH} is the data rate of TSCH in Kbps.

The frequency channel is idle for *TsTxAckDelay*, then followed by the transmission of an Ack (assuming that the data packet is correctly received by the intended receiver). The time duration in which the transmitter occupies the channel for Ack packet transmission denoted by T^a_{TSCH}, which is calculated as

$$T^a_{TSCH} = \frac{L^a_{TSCH} \times 8}{R_{TSCH}} \tag{11}$$

Accordingly, in a loop that traverses all timeslots, the model calculates the frequency channel that is used for transmission through (1). For each iteration of the loop, which represents one timeslot, $TsTxOffset/\delta$ elements of $TSCH_f$ and $TSCH_{tx}$ vectors are filled with zero, after that, T^d_{TSCH}/δ elements of $TSCH_f$ and $TSCH_{tx}$ are filled with derived frequency channels, and i_d, respectively. Continuing this, $TsTxAckDelay/\delta$ elements are filled with zero, and then T^a_{TSCH}/δ elements of $TSCH_f$, and $TSCH_{tx}$ are filled with derived frequency channels, and i_a, respectively. This procedure is repeated for all time steps in these vectors until it reaches the end of simulation. At the end, the model translates derived frequency channels to the actual RF frequencies by using (12).

$$f \leftarrow 2405 + 5 \cdot (f - 11)\ MHz,\ for\ f = 11...26 \tag{12}$$

The constants used in the model are extracted from the standard specification [2].

B. BLE time-frequency model

Following the same approach as for the TSCH model, we develop a model to extract the BLE frequency usage over time. This is done according to the BLE channel selection algorithm, node's behavior in the connection state, and the BLE packet structure. An overview of the inputs for the BLE channel usage model is given in Table. II. The T_{sim} and δ are also applied as inputs to the model with the same definition as described in the TSCH model.

Let BLE_f and BLE_{tx} be two vectors having $\lfloor T_{sim}/\delta \rfloor$ number of elements defined as follows.

$$\begin{aligned} &BLE_f = [f], \quad 1 \leq f \leq 37 \\ &BLE_{tx} = [indx], \quad indx = [0, i_d, i_a] \end{aligned} \tag{13}$$

where the element k $(1 \leq k \leq \lfloor T_{sim}/\delta \rfloor)$ of BLE_f indicates the frequency channel used for transmission at time $k \times \delta$ in case of transmission of data or Ack packets, otherwise is zero. The element k $(1 \leq k \leq \lfloor T_{sim}/\delta \rfloor)$ of BLE_{tx} indicates whether transmission is done by the data packet or Ack in time $k \times \delta$. Like in TSCH, i_d and i_a are used to indicate the transmission of data and Ack packets, respectively.

In the BLE model, per connection interval and for packets from one to *PPCI*, the channel selection algorithm derives a frequency channel according to (2). Then, it calculates the exact moments that the transmitter of the BLE occupies the channel by its transmission. The time durations for transmission of data and Ack packets in the occupied channel of BLE are denoted by T^d_{BLE} and T^a_{BLE}, respectively, which is calculated like (10), and (11). Between the packets, there is a period of *IPS*, during which the devices are idle.

We follow the same approach as for TSCH to fill the vectors of BLE_f and BLE_{tx} using the derived frequency channel for each connection interval, T^d_{BLE}, T^a_{BLE}, and *IPS*. Having BLE_f vector, the selected frequency channels (f) are mapped to the actual RF frequencies being occupied as follows.

$$f \leftarrow \begin{cases} 2404 + (f-1) \cdot 2\ MHz,\ for\ f = 1...11 \\ 2404 + f \cdot 2\ MHz,\ for\ f = 12...37 \end{cases} \tag{14}$$

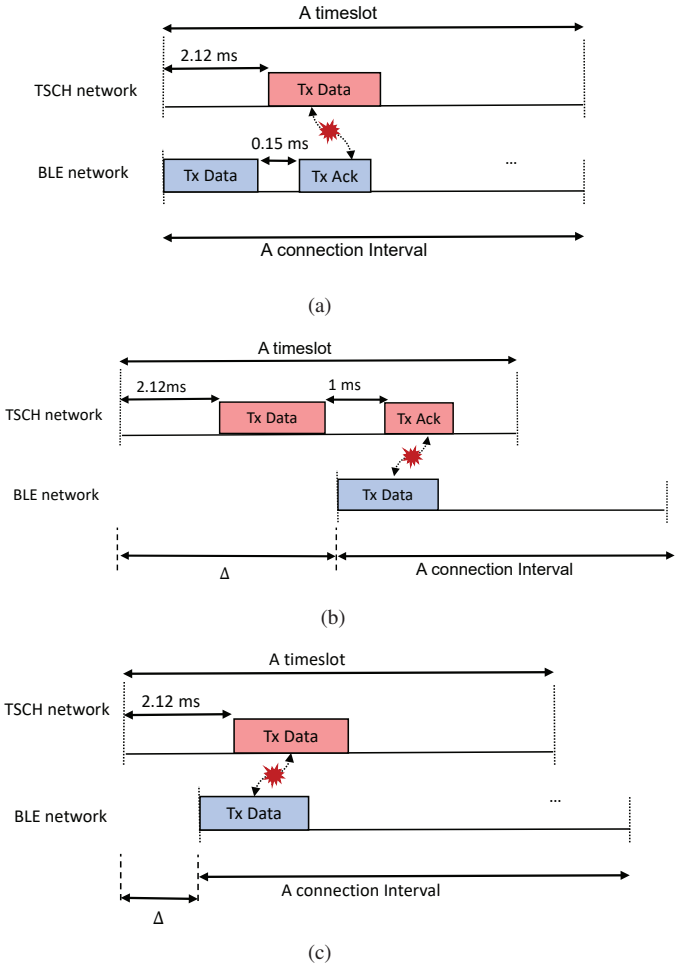

Fig. 6. Three examples of the scenarios in which TSCH and BLE packet transmissions overlap in time

C. Coexistence Model

The coexistence model uses the individual time-frequency models of TSCH and BLE to determine at what time and frequencies the TSCH and BLE devices transmit packets. Hence, it uses Δ and the outputs of both the BLE and TSCH models described in the previous sections. The models of TSCH and BLE are run separately in the coexistence model to derive $TSCH_f$, $TSCH_{tx}$, BLE_f, and BLE_{tx} vectors.

Fig. 6 shows three examples of time overlaps that may happen when co-located TSCH and BLE networks transmit in the overlapped frequency channels. Depending on the time-offset between the two networks, either data or Ack packets collide with one another. As shown in the figures, when data packets of either network collide, receiver nodes do not transmit any Ack packet. Thus, as an important step in the coexistence model, the output vectors are repaired.

Algorithm 1 describes the coexistence model. It uses TSCH and BLE models to get the $TSCH_f$, $TSCH_{tx}$, BLE_f, and BLE_{tx} vectors stated in lines 2-3. To apply Δ, $\lfloor|\Delta|/\delta\rfloor$ zeros are added to the front of the vectors of the network with later packet transmission. This process is stated in lines 5-10 of the algorithm. During a loop in line 13 iterating over time with steps of δ resolution, it examines whether a data packet transmission by the TSCH network overlaps in time and frequency domains by a transmission in the BLE network. If so, then data transmission by TSCH experiences a collision and, consequently, the corresponding Ack's values in $TSCH_f$, and $TSCH_{tx}$ should be replaced by zeros. The same procedure is done for BLE in the second loop starting from line 19. Table III lists all parameters that are used in the Algorithm.

TABLE III
PARAMETERS USED IN THE COEXISTENCE MODEL

Notation	Meaning
C_T^d	Counter that counts up when data in TSCH collides
C_T^a	Counter that counts up when Ack in TSCH collides
C_B^d	Counter that counts up when data in BLE collides
C_B^a	Counter that counts up when Ack in BLE collides
CFR_{TSCH}^{tx}	Collision-free ratio of TSCH in transmitter side (considering both data and Ack collisions)
CFR_{BLE}^{rx}	Collision-free ratio of TSCH in receiver side (considering only data collisions)
CFR_{TSCH}^{tx}	Collision-free ratio of BLE in transmitter side (considering both data and Ack collisions)
CFR_{BLE}^{rx}	Collision-free ratio of BLE in receiver side (considering only data collisions)

We define C_T^d, and C_T^a as the counter of the collisions of the data and Ack packets in the TSCH network, respectively. Similarly, C_B^d, and C_B^a are defined to count the number of collisions of the data and Ack packets in the BLE network, respectively. During a loop starting from line 27, if a data transmission in TSCH network collides with a transmission in the BLE network (data or Ack), the counter C_T^d is increased by one. Then, the loop index (k) is incremented by the time duration of the data packet transmission, that is expressed in line 31. If an Ack in TSCH experiences a collision, the counter C_T^a is increased by one, and loop index (k) is incremented by the time duration of the Ack transmission. We continue the same approach for BLE, and calculate C_B^d, and C_B^a during the fourth loop in line 37. Having that, we can derive collision-free ratios of BLE and TSCH from the receiver's point of view (denoted by CFR_{TSCH}^{rx} and CFR_{BLE}^{rx}) or transmitter's view (denoted by CFR_{TSCH}^{tx} and CFR_{BLE}^{tx}), in lines 46-47. Collision-free ratio from the receiver's point of view represents the reliability of the network in MAC, while collision-free ratio from transmitter's point of view reflects on the throughput and energy consumption affected by possible retransmissions caused by Ack failures.

For simplicity and without loss of generality, in this paper, we consider both fully and partially overlapped frequency channels as a collision. However, these cases can be separated in the Algorithm and counted as two different parameters.

D. Physical layer effects

The proposed coexistence model gives an insight into the probability of CTI between co-located TSCH and BLE networks in the MAC layer, providing collision-free communication ratios of both networks. Depending on the Signal to Interference and Noise Ratio (SINR) at the location of the intended receivers of these networks in the PHY layer, either of the collided packets in MAC layer may be correctly detected by the receiver. This can happen due to different transmission powers used by the nodes in TSCH and BLE networks, difference in the distance between the transmitter

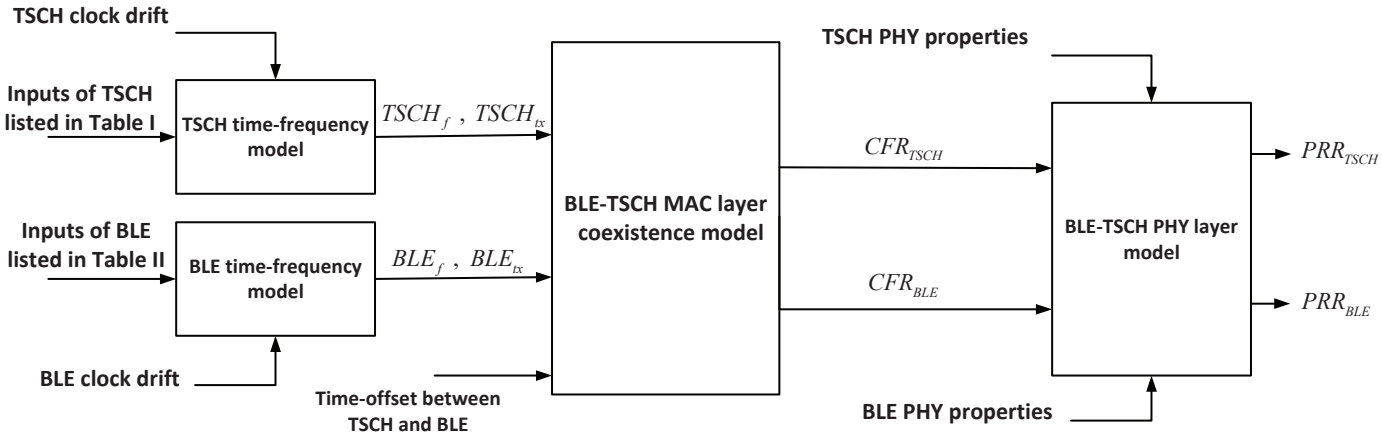

Fig. 7. The inputs and outputs of the BLE-TSCH coexistence simulator. The simulator results in MAC layer collision-free ratios, which is fed to PHY layer models to acquire packet reception ratio (PRR).

and the intended receiver, or the characteristics of the environment (path loss and multi-path fading effects) between the transmitter-receiver pairs. Even if all these parameters are the same for two TSCH and BLE networks, the differences of TSCH and BLE receivers such as modulation scheme can lead to successful delivery of a packet even when collision happens in the MAC layer. Therefore, the packet reception ratio measured in the PHY layer can be slightly higher than that of the MAC layer collision-free ratios provided by the coexistence model. Moreover, the packet reception ratio may be different for BLE and TSCH even if their collision-free ratios are the same in the MAC layer.

Note that when collisions happen in the partially-overlapped frequency channels, packet reception ratios are greater than when they happen in the fully-overlapped frequency channels, because of the signal strength related to the interference in the intended receiver side. As shown in Fig. 7, the outputs of the coexistence model can be fed to a PHY layer model, and finally derive the packet reception ratios of both networks. In this paper, we skip the PHY analysis, and focus on the MAC layers of the two networks, since existing works such [6] devoted to PHY layer analysis of TSCH and BLE that are plugged into the BLE-TSCH coexistence simulator.

VI. Experimental Model Verification

In this section, we aim to verify the developed simulation model by real-world experiments. We measure packet reception ratio from the receiver's point of view representing as collision-free ratio in PHY layer in various experimental settings. However, in a real-world experiments, packet receptions may be affected by SINR values in PHY layer, which leads to a small difference between packet reception ratio in PHY and collision-free ratio in the MAC layer. The results of the experiments are compared with the collision-free ratios derived from the simulation model for the same configuration settings.

We use the experimental setup shown in Fig. 8, composed of two co-located BLE and TSCH networks. The BLE network consists of two CC2650STK SensorTag [22] nodes, running a modified version of the TI BLE example of a Serial

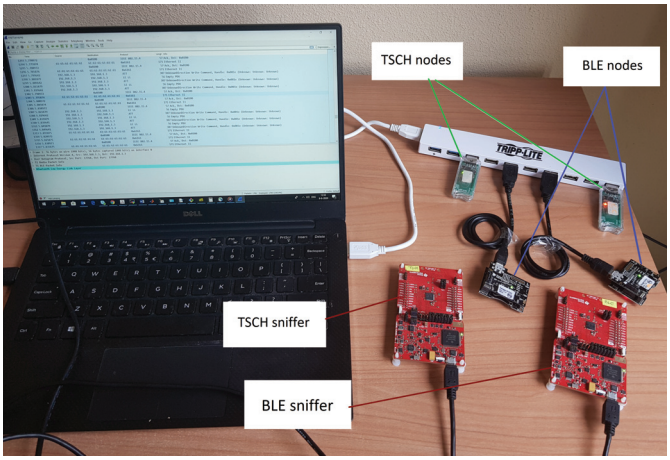

Fig. 8. Experimental setup for verification of the coexistence model

Port Profile (SPP) over BLE bridge designed for the CC2650 LaunchPad. The TSCH network contains two NXP JN5168 USB dongles [23], a PAN coordinator and an end-device. The JN5168 nodes run an application of the Contiki TSCH implementation [24], configured with no retransmissions, and $ChannelOffset = 0$. We set transmission power to 0 dBm in both TSCH and BLE networks.

When BLE enters to the connection state and intends to transmit its packets, a 'START' command is sent to TSCH through UART. The Contiki application running on the JN5168 USB dongle functioning as the PAN coordinator waits to receive the 'START' command from UART. It then starts transmission of one data packet per timeslot.

There can be extremely many settings, which cannot be controlled from the application layer. Thus, we need to know the specific settings in the real experiments and then apply the same settings to the simulator for comparison. The *ASN* and start time of the first data packet transmission in the TSCH network, *LUC, hI*, and start time of the first data packet transmission of the BLE network must be logged during the experiments. To do so, two TI CC2652R1 LaunchPad [25] boards are used as BLE and IEEE 802.15.4 sniffers. The sniffer devices are both connected directly to the laptop, on

Algorithm 1: BLE-TSCH coexistence simulation model

Main ()
  $TSCH_f, TSCH_{tx} \leftarrow$ **TSCH model** $(TSCH_f, TSCH_{tx})$
  $BLE_f, BLE_{tx} \leftarrow$ **BLE model** (BLE_f, BLE_{tx})
  /* Add zeros to the beginning of the vectors of later network */
  if *TSCH is later* **then**
    $[[0]_{\lfloor|\Delta|/\delta\rfloor}, TSCH_f]$
    $[[0]_{\lfloor|\Delta|/\delta\rfloor}, TSCH_{tx}]$
  else
    $[[0]_{\lfloor|\Delta|/\delta\rfloor}, BLE_f]$
    $[[0]_{\lfloor|\Delta|/\delta\rfloor}, BLE_{tx}]$
  /* Check if data packets transmission collide, remove corresponding Ack */
  k=1
  while $k \leq \lfloor T_{sim}/\delta \rfloor$ **do**
    if $|TSCH_f(k) - BLE_f(k)| \leq 1MHz$ **then**
      if $TSCH_{tx}(k) == i_d$ **then**
        replace the corresponding Ack with 0
      $k = k + \lfloor T^d_{TSCH}/\delta \rfloor$
  k=1
  while $k \leq \lfloor T_{sim}/\delta \rfloor$ **do**
    if $|TSCH_f(k) - BLE_f(k)| \leq 1$ MHz **then**
      if $BLE_{tx}(k) == i_d$ **then**
        replace the corresponding Ack with 0
      $k = k + \lfloor T^d_{BLE}/\delta \rfloor$
  $C^d_T = 0, \quad C^a_T = 0\,, \quad C^d_B = 0, \; C^a_B = 0$
  /* Check if data (or Ack) packets of TSCH collide, increment C^d_T (or C^a_T) by one */
  k=1
  while $k \leq \lfloor T_{sim}/\delta \rfloor$ **do**
    if $|TSCH_f(k) - BLE_f(k)| \leq 1$ MHz **then**
      if $TSCH_{tx}(k) == i_d$ **then**
        $C^d_T = C^d_T + 1$
        $k = k + \lfloor T^d_{TSCH}/\delta \rfloor$
      else if $TSCH_{tx}(k) == i_a$ **then**
        $C^a_T = C^a_T + 1$
        $k = k + \lfloor T^a_{TSCH}/\delta \rfloor$
  /* Check if data (or Ack) packets of BLE collide, increment C^d_B (or C^a_B) by one */
  k=1
  while $k \leq \lfloor T_{sim}/\delta \rfloor$ **do**
    if $|TSCH_f(k) - BLE_f(k)| \leq 1$ MHz **then**
      if $BLE_{tx}(k) == i_d$ **then**
        $C^d_B = C^d_B + 1$
        $k = k + \lfloor T^d_{BLE}/\delta \rfloor$
      else if $BLE_{tx}(k) == i_a$ **then**
        $C^a_B = C^a_B + 1$
        $k = k + \lfloor T^a_{BLE}/\delta \rfloor$

  $CFR^{rx}_{TSCH} = 1 - \frac{C^d_T}{\lfloor T_{sim}/T_{ts} \rfloor}$, $CFR^{tx}_{TSCH} = 1 - \frac{C^d_T + C^a_T}{\lfloor T_{sim}/T_{ts} \rfloor}$

  $CFR^{rx}_{BLE} = 1 - \frac{C^d_B}{\lfloor T_{sim}/T_{ci} \rfloor}$, $CFR^{tx}_{BLE} = 1 - \frac{C^d_B + C^a_B}{\lfloor T_{sim}/T_{ci} \rfloor}$

which TI's SmartRF Packet Sniffer is used to configure and forward their gathered data to Wireshark [26]. Channel 39 in BLE is used to advertise, and the BLE sniffer scans this channel. The BLE sniffer is setup to follow the connections of the BLE master. The IEEE 802.15.4 sniffer is set to monitor channel 11 of TSCH. Through analysis of the captured data by Wireshark, we derive the values of parameters *ASN*, *LUC*, *hI*, and Δ. By applying these inputs to the simulation model, we derive collision-free ratios, and compare with the experiments results.

Setting \ Scenario	1	2	3	4	5	6
L^d_{TSCH} (byte)	133	79	133	79	133	79
L^d_{BLE} (byte)	261	261	139	139	78	78
Δ (μs)	9510	4760	2730	6010	2220	4010

(a) Packet length of TSCH and BLE for each scenario

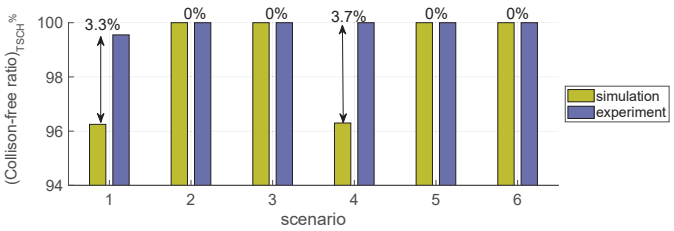

(b) Collision-free ratio of TSCH network

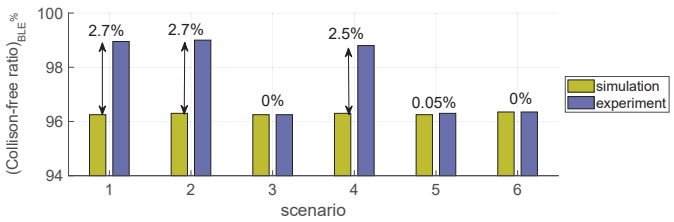

(c) Collision-free ratio of BLE network

Fig. 9. Simulation and experiment results for collision-free ratios of TSCH and BLE with different packet length

All experiments are conducted in an interference-free isolated room to prevent uncontrolled external interference. We set $T_{sim} = 20s$, $\delta = 10\mu s$, $PPCI = 1$, $L^a_{TSCH} = 19$, and $L^a_{BLE} = 10$ in all experiments. Furthermore, TSCH is the later network for transmission of the first data packet in all experiments. Although, the experiments are performed with two nodes in each network, in which the transmitter node transmits in all TSCH timeslots (or BLE connection intervals), it can be considered as several transmitter nodes in both networks that transmit data packets in their own scheduled timeslot (or connection interval) according to the TSCH schedule (or management of the master node in BLE). In all experiments and simulations, we force the TSCH and BLE networks to use their full bandwidth by performing packet transmission in all timeslots or connection intervals to be able to study the worst-case coexistence scenario. This full bandwidth usage can be considered to be done by any number of nodes in that neighborhood.

In the first experiment, we consider six scenarios in which different packet lengths for TSCH and BLE are set. In this experiment, we set $T_{ts} = T_{ci} = 10ms$, and use all available channels of TSCH and BLE. Results derived from the simulation model and experiments are presented in Fig.9. The packet length settings and Δ that are measured for each scenario are stated in Fig. 9(a). The first observation is that Δ is important for coexistence of these networks. For instance, Δ is $9510\mu s$ in scenario 1, meaning that their data packet transmissions collide with each other if their transmissions happen in the overlapped frequency channels. This is why the collision-free ratios are less than 100% in both networks. In scenario 2, Δ is $4760\mu s$, meaning that TSCH transmits its data packets in the idle time of the connection interval of BLE, and thus can deliver its data packets without collision despite the overlap

Setting \ Scenario	1	2	3	4	5	6
T_{ts} (ms)	10	10	10	15	15	15
T_{ci} (ms)	10	12.5	15	10	12.5	15
Δ (μs)	510	6600	11670	940	790	830

(a) T_{ts} and T_{ci} for each scenario

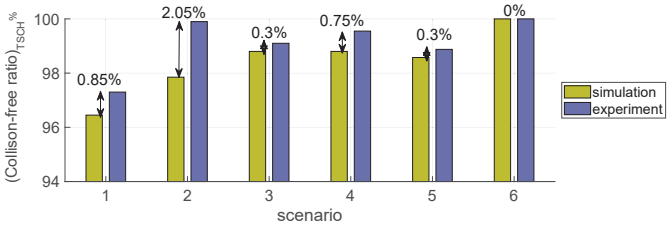

(b) Collision-free ratio of TSCH network

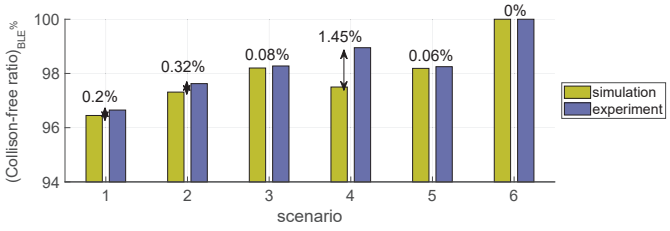

(c) Collision-free ratio of BLE network

Fig. 10. Simulation and experiment results for collision-free ratios of TSCH and BLE with different T_{ts} and T_{ci}

Setting \ Scenario	1	2	3
HSL	[11:26]	[11:26]	[11,13,15,17, 19,21,23,25]
ChM	[1:37]	[3,5,8,10,12, 14,17,19,22,24, 27,29,32,34,37]	[1:37]
Δ (μs)	7420	8130	2610

(a) HSL and ChM for each scenario

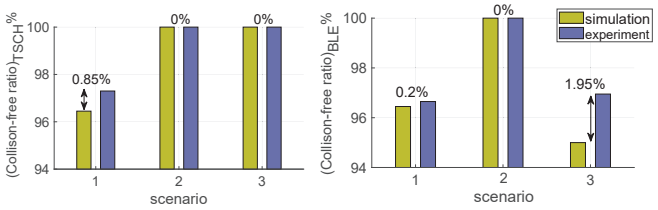

(b) Collision-free ratio of TSCH (c) Collision-free ratio of BLE

Fig. 11. Simulation and experiment results for collision-free ratios of TSCH and BLE for different *HSL* and *ChM*

in frequency domain. This holds even when Ack packets of TSCH collide with transmissions of the data packets in BLE, if both networks transmit in the overlapped frequency channels. So, collision-free ratio of TSCH is 100%, while collision-free ratio of BLE is less than 100%.

The second observation is that the simulation results are slightly lower than the measured ones in the corresponding experiment. As we discussed, this happens when collision-free ratio is less than 100%, and the collided packets in the MAC layer are received by the intended receiver because of their higher SINR values in the PHY layer, while they are counted as collisions in the simulation model. The third observation is that the difference between simulation results and experiments for TSCH is more than that for BLE. It means that, the TSCH receiver could better detect collided packets compared to the BLE receiver, resulting in TSCH to be less affected by interference (BLE transmission) than vice versa. The reason is the known difference between PHY layers of TSCH and BLE such as the gain of the DSSS process (around 9 dB) in the TSCH network [6], which comes at the cost of lower channel efficiency (lower bit rate) for this technology.

In the second experiment, we consider six scenarios in which different T_{ts} and T_{ci} are set with packet length settings as $L^d_{TSCH} = 133$, and $L^d_{BLE} = 261$. All available channels of TSCH and BLE are used. Fig. 10 shows collision-free ratios for all scenarios whose settings and Δ are reported in Fig. 10(a). As shown, the experiment results track the simulation results with acceptable error whose source is discussed in the first experiment.

To have a more extensive verification of the simulation model, we also investigate the accuracy of the coexistence simulator when either network uses channel blacklisting. To do so, we consider three scenarios as follows. First, we use all available channels for TSCH and BLE. Second, BLE performs blacklisting and uses only the channels that do not overlap with TSCH channels. In the third scenario, TSCH conducts blacklisting by removing the fully-overlapped channels and using only partially-overlapped channels. In Fig. 11(a), *HSL*, *ChM*, Δ for all scenarios in this experiment are listed in the table. Collision-free ratios of TSCH and BLE are illustrated in Fig. 11 for these scenarios. We set $T_{T_{ts}} = T_{ci} = 10ms$, $L^d_{TSCH} = 133$, and $L^d_{BLE} = 261$. As we expected, collision-free ratios of TSCH and BLE for the second scenario are 100% regardless of time overlap, since BLE performs blacklisting by selecting only non-overlapped frequency channels.

Comparing the results for all experiments, it is revealed that the simulation results are either equal, or slightly lower than the experimental results. Hence, our proposed model can be used to conservatively estimate the collision-free ratio with an acceptable accuracy.

VII. Worst-case coexistence analysis

The worst-case coexistence analysis gives insights into the extent to which the coexisting networks can deteriorate each others performance. It helps the network designers to prepare for such scenarios and, if needed, fortify their networks with mechanisms to avoid getting trapped in the worst-case scenarios. Thanks to the fast coexistence simulator developed in this work, we can run Monte-Carlo simulations for many coexistence scenarios to detect (near-)worst cases. Here, we investigate the worst-case scenarios when both networks use all available channels for channel hopping ($ChM = [1:37]$, $HSL = [11:26]$). We use $L^d_{BLE} = 261$, $L^d_{TSCH} = 133$, and $T_{ci} = T_{ts} = 10ms$ in the coexistence simulation model, because the minimum connection interval of BLE is 10ms [1], and the default value of timeslot length in TSCH is 10ms [2]. As discussed, *hI* is selected by the master node randomly in range of [5 16]. Also, the first channels selected by TSCH and BLE for transmission of the first data packets and the order of the frequency channels in *HSL* and *ChM* can be varied. Depending on these settings, $12 \times 16 \times 37 \times 16! \times 37!$ scenarios can happen, in which overlaps in frequency domain for successive packet transmissions may be different. Exhaustive search in such a large set of settings is impossible. To have reliable enough exploration and thanks to the speed of this coexistence simulator, we try 10^6 random settings selected

from all possible settings with different T_{sim}. It turned out that, when we fairly set the simulation time, in such a way so that all possible combinations of TSCH and BLE packet transmissions in each channel happens, collision-free ratios measured with different settings are the same. It is regardless of which *hI* value or channel sequences are selected by TSCH and BLE for data packet transmission. Hence, we set $T_{sim} = (16 \times 37 \times 10)ms$. Note that, all combinations of transmission by TSCH and BLE in different channels will happen if this particular number ($|HSL| \times |ChM|$) or multiple of this number of channel hopping is iterated in the simulation.

Two parameters that can affect the coexistence performance are *PPCI* and Δ. We run the coexistence simulator for possible values of *PPCI* and Δ. Since we set $T_{ci} = 10ms$, at most 4 packets can be transmitted with maximum packet length during the connection interval. Tables. IV and V report collision-free ratios of TSCH and BLE for different *PPCI* and Δ. Comparing the results in the tables, it is observed that more packets transmitted in the connection interval results in higher chance of collision in the TSCH network. It in turn leads to lower collision-free ratios of TSCH. However, this trend depends on the value of Δ. For instance, when $\Delta = 0$ *or* $\geq$ 8ms, collision-free ratios of TSCH is 96.29%, regardless of *PPCI* value. In these cases, only one of the BLE packets in the connection interval is collided with the TSCH data packet. Fig. 12 shows channel occupancy of BLE and TSCH over time for the first 100 packets, when $PPCI = 1$, and $\Delta = 8ms$. It is illustrated that 9 out of 100 transmitted data packets in TSCH and BLE are collided.

Collision-free ratio of TSCH goes down to 92.58% in the worst-case when Δ is in the range of 4 to 7ms. Setting these Δ values increases the chance of time-overlapping of data packets. The worst-case in BLE (96.29%) happens when one or two packets are transmitted per connection interval, and Δ is more than 3ms.

Outcomes of the worst-case analysis are:

- TSCH and BLE can coexist with satisfying performance even in worst-case scenarios (collision-free ratio of TSCH $\geq$ 92.58%, and collision-free ratio of BLE $\geq$ 96.29%), since both networks use channel hopping.
- When Δ is close to the middle of connection interval, more packets are collided with transmission by the TSCH network. So, an appropriate way of cooperatively synchronizing the two networks can improve their coexistence performance.

VIII. Impact of Clock Drift

The TSCH and BLE networks have continuously running synchronization processes to keep the nodes aligned despite the clock drifts caused by oscillator variations. However, the timing of co-located TSCH and BLE networks with respect to one another (Δ) may change over time due to clock drifts within each network. To investigate this fact, clock drifts of two networks are applied as inputs to the coexistence model. Here, we perform two set of simulations to observe how clock drift may change collision-free ratios over time. The settings are as $L^d_{BLE} = L^d_{TSCH} = 70$, and $T_{ci} = T_{ts} = 10ms$. Typical clock drift of $\pm 50ppm$ for the crystal oscillator is considered [1], which leads to a mutual drift of maximum 1μs per each 10ms. Thus, Δ may change at most 1μs after each 10ms. Accordingly, cumulative drift changes time overlap of the networks within the time window under observation. To show the possible impact, we zoom into two special simulation time durations in which the cumulative drift improve, or degrade the collision-free ratios over time. In the first scenario, it is assumed that BLE is 1.31ms later than TSCH ($\Delta = -1.31ms$), which leads to no overlap in time domain. After a while cumulative drift increases causing Ack of BLE to overlap with TSCH data packets. Fig. 13(a) shows the collision-free ratios of two networks over time. After 260ms (corresponding to the 26 packet transmissions), the collision-free ratio of TSCH decreases from 100% to lower values depending on the number of collided channels, but the

TABLE IV
COLLISION-FREE RATIO OF TSCH%

Δ(ms) \ PPCI	1	2	3	4
0	96.29	96.29	96.29	96.29
1	100	96.29	96.29	96.29
2	100	96.29	96.29	96.29
3	100	100	96.29	96.29
4	96.29	96.29	**92.58**	**92.58**
5	96.29	96.29	**92.58**	**92.58**
6	96.29	96.29	96.29	**92.58**
7	96.29	96.29	96.29	**92.58**
8	96.29	96.29	96.29	96.29
9	96.29	96.29	96.29	96.29

TABLE V
COLLISION-FREE RATIO OF BLE%

Δ(ms) \ PPCI	1	2	3	4
0	100	98.15	97.53	98.15
1	100	98.15	97.53	98.15
2	100	98.15	97.53	97.22
3	**96.29**	98.15	97.53	97.22
4	**96.29**	98.15	97.53	97.22
5	**96.29**	98.15	98.76	98.15
6	**96.29**	98.15	98.76	98.15
7	**96.29**	**96.29**	97.53	97.22
8	**96.29**	**96.29**	97.53	98.15
9	**96.29**	**96.29**	**96.29**	97.22

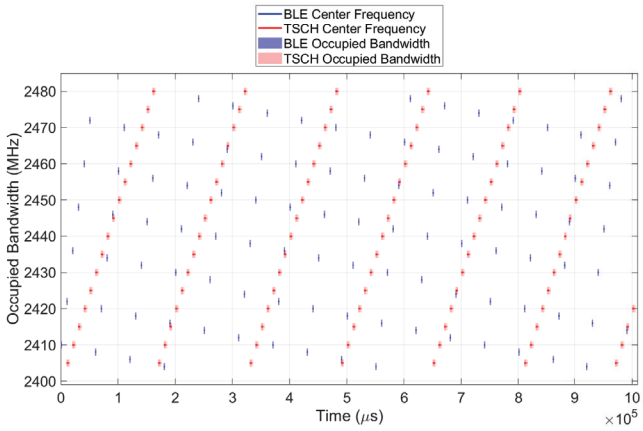

Fig. 12. Channel occupancy of BLE and TSCH over time for 1s ($\simeq$100 data packets transmission)

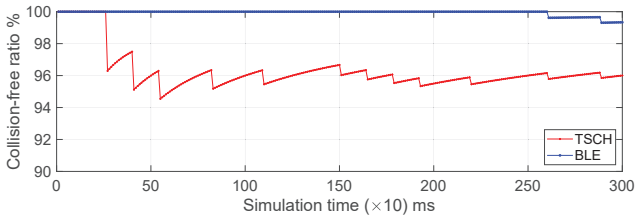

(a) Degradation of coexistence performance over time due to clock drifts in BLE and TSCH networks

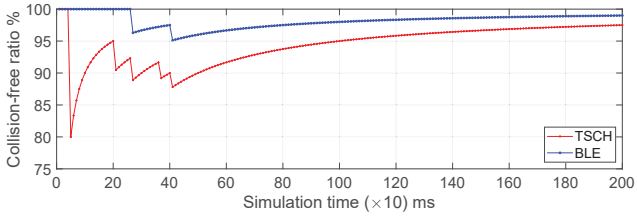

(b) Improvement in coexistence performance over time due to clock drifts in BLE and TSCH networks

Fig. 13. Impact of clock drift on BLE-TSCH coexistence performance

collision-free ratio of BLE is still 100%. This trend continues until the cumulative drift makes BLE data packets overlap with TSCH data packets, degrading the BLE performance as well.

In the second scenario, we consider an opposite situation, in which the time-offset makes two networks overlapping in time at the beginning, but clock drift takes the networks out of this situation after a while. We consider BLE is 4.31ms later than TSCH ($\Delta = -4.31ms$), causing time overlap. Thus, data packets of the two networks collide when they transmit in the overlapped frequency channels. Fig. 13(b) illustrates the collision-free ratios of the two networks. After 400ms, their mutual drift takes the networks out of the situation. Accordingly, the collision-free ratio increase for both networks.

IX. Conclusion

In this paper, we investigate the coexistence of co-located BLE and IEEE 802.15.4 TSCH networks. A probabilistic analysis of collision-free communications in the MAC layer for coexisting BLE and TSCH is presented. Also, simulation models for TSCH and BLE are derived, which output frequency channel usage over time. We analyze the collisions occurrence through the derived TSCH and BLE models. Based on that, a simulation model is developed for the coexistence of TSCH and BLE in the MAC layer. To verify the simulation model, we provide an experimental evaluation of co-located BLE and TSCH in an isolated room. The experimental results are slightly higher than the simulation results (maximum difference is 3.7%) due to physical layer effects. Thus, our simulation model conservatively estimates collision-free ratio with an acceptable accuracy. Using the coexistence model, worst-case performance of co-located TSCH and BLE is studied. The results show that TSCH and BLE can coexist very well even in the worst-case scenarios with collision-free ratios of TSCH and BLE being more than 92.58% and 96.29%, respectively.

References

[1] "Specification of the Bluetooth System, v4.2," *Bluetooth SIG*, pp. 1–2772, December 2014.
[2] "IEEE Standard for Low-Rate Wireless Networks," *IEEE Std 802.15.4-2015 (Revision of IEEE Std 802.15.4-2011)*, pp. 1–709, April 2016.
[3] P. Tiwari, V. Saxena, R. Mishra, and D. Bhavsar, "Wireless Sensor Networks: Introduction, Advantages, Applications and Research Challenges," *HCTL Open International Journal of Technology Innovations and Research (IJTIR)*, vol. 14, 05 2015.
[4] A. Elsts, X. Fafoutis, G. Oikonomou, R. Piechocki, and I. Craddock, "TSCH Networks for Health IoT: Design, Evaluation, and Trials in the Wild," *ACM Trans. Internet Things*, vol. 1, no. 2, Apr. 2020. [Online]. Available: https://doi.org/10.1145/3366617
[5] P. Narendra, S. Duquennoy, and T. Voigt, "BLE and IEEE 802.15. 4 in the IoT: Evaluation and Interoperability Considerations," in *International Internet of Things Summit*. Springer, 2015, pp. 427–438.
[6] R. Natarajan, P. Zand, and M. Nabi, "Analysis of coexistence between IEEE 802.15.4, BLE and IEEE 802.11 in the 2.4 GHz ISM band," in *IECON 2016 - 42nd Annual Conference of the IEEE Industrial Electronics Society*, Oct 2016, pp. 6025–6032.
[7] O. Carhacioglu, P. Zand, and M. Nabi, "Cooperative Coexistence of BLE and Time Slotted Channel Hopping Networks," in *2018 IEEE 29th Annual Int'l Symp. Personal, Indoor and Mobile Radio Communications (PIMRC)*, Sep. 2018, pp. 1–7.
[8] F. Osterlind, A. Dunkels, J. Eriksson, N. Finne, and T. Voigt, "Cross-Level Sensor Network Simulation with COOJA," in *Proceedings. 2006 31st IEEE Conference on Local Computer Networks*, 2006, pp. 641–648.
[9] Z. Bojthe, L. Meszaros, and A. Varga, INET Framework. [Online]. Available: https://inet.omnetpp.org.
[10] M. Woolley, "Bluetooth Core Specification v5." 2019.
[11] B. Kim, J. Choi, and J. Cho, "A Hybrid Channel Access Scheme for Coexistence Mitigation in IEEE 802.15.4-Based WBAN," *IEEE Sensors Journal*, vol. 17, no. 21, pp. 7189–7195, 2017.
[12] B. Lu, Z. Qin, Y. Sun, J. Hu, and L. Wang, "A Dynamic Self-Adapting Mechanism for ZigBee Performance Assurance Under Wi-Fi Interference," *IEEE Sensors Journal*, vol. 18, no. 9, pp. 3900–3909, 2018.
[13] S. Ben Yaala, F. Theoleyre, and R. Bouallegue, "Performance study of co-located IEEE 802.15.4-TSCH networks: Interference and coexistence," in *2016 IEEE Symposium on Computers and Communication (ISCC)*, June 2016, pp. 513–518.
[14] A. Hithnawi, H. Shafagh, and S. Duquennoy, "Understanding the Impact of Cross Technology Interference on IEEE 802.15.4," in *Proceedings of the 9th ACM International Workshop on Wireless Network Testbeds, Experimental Evaluation and Characterization*, ser. WiNTECH '14. New York, NY, USA: ACM, 2014, pp. 49–56. [Online]. Available: http://doi.acm.org/10.1145/2643230.2643235
[15] V. Waghmare and R. Deshmukh, "Bluetooth and Wi-Fi : Coexistence Issues and Solutions Review," 10 2009.
[16] S. Zacharias, T. Newe, S. O'Keeffe, and E. Lewis, "Coexistence measurements and analysis of IEEE 802.15.4 with Wi-Fi and Bluetooth for vehicle networks," in *2012 12th Int'l Conf. on ITS Telecommunications*, Nov 2012, pp. 785–790.
[17] NXP Semiconductors, "Co-existence of IEEE 802.15.4 at 2.4 GHz - Application Note," Tech. Rep. JN-AN-1079, November 2013, https://www.nxp.com/docs/en/application-note/JN-AN-1079.pdf.
[18] ——, "IEEE 802.15.4 and BLE Coexistence Performance," Tech. Rep. KW41Z, August 2018, https://www.nxp.com/docs/en/application-note/AN12231.pdf.
[19] M. Chwalisz and A. Wolisz, "Towards efficient coexistence of IEEE 802.15.4e TSCH and IEEE 802.11," in *NOMS 2018 - 2018 IEEE/IFIP Network Operations and Management Symposium*, April 2018, pp. 1–7.
[20] J. Lustig (2018), "Coexistence Between BLE and IEEE 802.15.4 Networks," KTH, Sweden.
[21] F. Veisi, M. Nabi, and H. Saidi, "Coexistence Analysis of Multiple Asynchronous IEEE 802.15.4 TSCH-based Networks," *IEEE Access*, vol. 8, pp. 150 573–150 585, 2020.
[22] Texas Instruments. CC2640/CC2650 Bluetooth low energy Software Developers Guide (Rev. E). http://www.ti.com/lit/ug/swru393e/swru393e.pdf.
[23] NXP Semiconductors, "JN516x IEEE802.15.4 Wireless Microcontroller," accessed: Sept. 2017.
[24] A. Dunkels, B. Gronvall, and T. Voigt, "Contiki- a lightweight and flexible operating system for tiny networked sensors," in *29th annual IEEE international conference on local computer networks*. IEEE, 2004, pp. 455–462.

[25] Texas Instruments. SmartRF Packet Sniffer 2 v1.70. http://www.ti.com/tool/download/PACKET-SNIFFER-2.
[26] Wireshark. Wireshark. https://www.wireshark.org/.

Hamideh Hajizadeh received the B.Sc. degree in electronics engineering, and the M.Sc. degree in communication systems engineering both from Tehran University. She is currently working towards her Ph.D. in electrical and computer engineering at the Eindhoven University of Technology (TU/e), Eindhoven, the Netherlands.

Majid Nabi (S08-M13) received the B.Sc. and M.Sc. degrees both in computer engineering from Isfahan University of Technology and Tehran University, respectively. He received the Ph.D. degree in electrical and computer engineering from Eindhoven University of Technology (TU/e), Eindhoven, the Netherlands in 2013. He is currently an assistant professor with the Department of Electrical Engineering at TU/e, and Isfahan University of Technology. His research interests include efficient and reliable networked embedded systems, low-power wireless sensor networks, and internet-of-things. He is a member of IEEE.

Maik Vermeulen received the B.Sc. degree in electrical engineering in 2017, and the M.Sc. degree in embedded systems in 2019 both from Eindhoven University of Technology. He is currently working at InnoTractor in Tilburg, developing IoT devices mainly focused on the next revolution in logistics.

Kees Goossens has a BSc in computer science from the University of Wales (1988), and a PhD from the University of Edinburgh (1993). In his thesis he investigated the formal verification of hardware, in particular by using semi-automated proof systems in conjunction with formal semantics of hardware description languages such as ELLA and VHDL. He continued this work at several other universities before joining Philips Research in the Netherlands in 1995. At Philips he worked on behavioural synthesis for high-throughput video processing, then on on-chip communication protocols and memory management. Until 2010, at Philips/NXP Semiconductors Research he led the team that defined the Aethereal network on chip for consumer electronics, where real-time performance and low cost are major constraints. He was also part-time full professor at the Delft University of Technology from 2007 to 2010, and is currently full professor at the Eindhoven University of Technology, where his research focusses on composable (virtualised), predictable (real-time), low-power embedded systems, supporting multiple models of computation. He is also system architect at Topic Embedded Products, working on real-time dependable dynamic partial reconfiguration in FPGAs. He is editorial board member for the ACM Transactions on Design Automation of Electronic Systems (TODAES), associate editor for the Springer Journal of Design Automation of Embedded Systems (DAEM), and was guest editor for several special issues on networks on chip. He is author on 25 patents, and published four books, 100+ articles, with four paper awards. His 2003 paper was selected as one of the 30 most influential papers of 10 years of the DATE conference. He is or was steering committee member of ACSD, NOCS, MPSOC, and TPC member of CODES+ISSS, CRTS, DATE, DSD, ECRTS, FPL, ICPP, INA-OCMC, OMHI, NoCArc, PARMA, QVVP, ReConFig, RTAS, SAMOS, SDR, SOC, and VLSI-SOC, etc.